Inorg. Chem. **2007**, *46*, 1817–1824

Cobaloximes as Functional Models for Hydrogenases. 2. Proton Electroreduction Catalyzed by Difluoroborylbis(dimethylglyoximato)cobalt(II) Complexes in Organic Media

Carole Baffert, Vincent Artero,* and Marc Fontecave

Laboratoire de Chimie et Biologie des Métaux, Université Joseph Fourier, CNRS, UMR 5249, and CEA, DSV/iRT SV/LCBM, 38054 Grenoble, France

Received August 29, 2006

Cobaloximes are effective electrocatalysts for hydrogen evolution and thus functional models for hydrogenases. Among them, difluoroboryl-bridged complexes appear both to mediate proton electroreduction with low overpotentials and to be quite stable in acidic conditions. We report here a mechanistic study of $[Co(dmgBF_2)_2L]$ (dmg^{2-} = dimethylglyoximato dianion; L = CH_3CN or *N*,*N*-dimethylformamide) catalyzed proton electroreduction in organic solvents. Depending on the applied potential and the strength of the acid used, three different pathways for hydrogen production were identified and a unified mechanistic scheme involving cobalt(II) or cobalt(III) hydride species is proposed. As far as working potential and turnover frequency are concerned, $[Co(dmgBF_2)_2(CH_3CN)_2]$, in the presence of *p*-cyanoanilinium cation in acetonitrile, is one of the best synthetic catalysts of the first-row transition-metal series for hydrogen evolution.

Introduction

In the perspective of a hydrogen economy, one major issue concerns the availability of economically viable methods for the production of hydrogen from renewable sources. The reduction of protons is apparently a very simple reaction but, unfortunately, except on platinum metal electrodes, suffers from kinetic limitations. On most electrodes, the rate-determining step is the heterogeneous electron transfer from the electrode to a proton located in the solution, resulting in the formation of a hydride ion stabilized at the surface. The reaction of this hydride with a proton from the bulk is fast. Hence, on common and inexpensive solid materials, hydrogen evolution is generally not observed at potentials near equilibrium (−400 mV vs SHE at pH 7 in water) but requires the application of an overpotential, also called an activation potential.[1] Hydrogenases are unique metalloenzymes that catalyze the reversible H_2/H^+ interconversion.[2] When adsorbed on a glassy carbon electrode, [NiFe] hydrogenase from *Allochromatium vinosum* displays a Nernstian catalytic behavior for H_2/H^+ interconversion[3] and appears thus competitive as an efficient molecular catalyst with regard to platinum for the hydrogen evolution reaction (*her*). Concurrently, the development of new homogeneous catalysts for *her* based on cheap first-row transition metals has been a long-time goal for inorganic chemists.[4] The final goal lies in an alternative to the use of platinum as the electrode for this reaction by modifying a common electrode material with a molecular complex able to catalyze the reaction, i.e., to lower the activation potential for *her*. Significant achievements have been reported in the past years in the structural modelization of hydrogenases,[5] but the new biomimetic models show activities still below those obtained with non-biomimetic synthetic catalysts such as $[Ni(P^{Ph}{}_2N^{Ph}{}_2)_2(CH_3CN)](BF_4)_2$ ($P^{Ph}{}_2N^{Ph}$ = 1,3,5,7-tetraphenyl-1,5-diaza-3,7-diphosphacyclooctane),[6] $[Cp_2Mo_2(\mu\text{-}S)_2(\eta^2\text{-}\mu_2\text{-}CH_2S_2)]$,[7] or $[Cp^*Rh(bipy)(OH_2)]^{2+}$.[8]

* To whom correspondence should be addressed. E-mail: vartero@cea.fr. Phone: int+ 4 38 78 91 06. Fax: int+ 4 38 78 91 24.

(1) The same occurs for hydrogen oxidation. This kinetic limitation thus significantly reduces the energetic yield during a complete formation/uptake cycle of hydrogen and is therefore economically limitating for most industrial applications.

(2) (a) Adams, M. W. W.; Mortenson, L. E.; Chen, J.-S. *Biochim. Biophys. Acta* **1981**, *594*, 105. (b) Vignais, P. M.; Billoud, B.; Meyer. *J. FEMS Microbiol. Rev.* **2001**, *25*, 455.

(3) (a) Jones, A. K.; Sillery, E.; Albracht, S. P. J.; Armstrong, F. A. *Chem. Commun.* **2002**, 866. (b) Pershad, H. R.; Duff, J. L. C.; Heering, H. A.; Duin, E. C.; Albracht, S. P. J.; Armstrong, F. A. *Biochemistry* **1999**, *38*, 8992. (c) Léger, C.; Jones, A. K.; Roseboom, W.; Albracht, S. P. J.; Armstrong, F. A. *Biochemistry* **2002**, *41*, 15736.

(4) (a) Artero, V.; Fontecave, M. *Coord. Chem. Rev.* **2005**, *549*, 1518. (b) Koelle, U. *New J. Chem.* **1992**, *16*, 157.

10.1021/ic061625m CCC: $37.00
Published on Web 02/02/2007

Chart 1. $[Co(dmgBF_2)_2L_2]$ (L = H_2O, CH_3CN, or DMF)

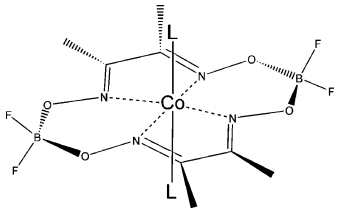

Cobaloxime is another class of such catalysts. The first report concerned the reduction of protons by MCl_2 (M = V, Cr, Eu) at pH 2 in water catalyzed by $[Co(dmgBF_2)_2(OH_2)_2]$ [$dmgBF_2^-$ = (difluoroboryl)dimethylglyoximato anion; Chart 1].[9] Lehn et al. also described the photoproduction of hydrogen at pH 8 in *N*,*N*-dimethylformamide (DMF) catalyzed by $[Co(dmgH)_2(OH_2)_2]$ in the presence of a photosensitizer $[Ru(bipy)_3]^{2+}$ and sacrificial triethanolamine as the electron donor.[10] We recently reported on the activity of various cobaloximes[11] as electrocatalysts for the reduction of a weak acid, Et_3NH^+, in DMF or 1,2-dichloroethane and demonstrated that the active species is a cobalt(III) hydride formed by protonation of the Co^I complex. We also concluded that $[Co(dmgBF_2)_2(OH_2)_2]$ is a slow electrocatalyst under these conditions even at a potential 350 mV more negative than that required for Co^I formation. Soon after, this complex was shown to behave electrocatalytically at the Co^I redox state in the presence of stronger acids such as HBF_4 or CF_3COOH in acetonitrile.[12] In order to determine whether this difference in reactivity implies a distinct catalytic mechanism or simply reflects kinetic limitations, we thus decided to reinvestigate $[Co(dmgBF_2)_2L]$-catalyzed proton electroreduction in both DMF and CH_3CN, using a variety of acids with different pK_a's and extending the electrochemical window toward the reduction region. Interestingly, three different pathways for hydrogen production could be identified, depending on the strength of the acid used, and we propose here a unified mechanistic scheme for hydrogen production involving cobalt(II) or cobalt(III) hydride.

Experimental Section

Materials. Commercial DMF and acetonitrile were degassed by bubbling nitrogen. The supporting electrolyte $(n\text{-}Bu_4N)BF_4$ was prepared from $(n\text{-}Bu_4N)HSO_4$ and $NaBF_4$ (Aldrich) and dried overnight at 80 °C under vacuum. $[Co(dmgBF_2)_2(OH_2)_2]$,[13] $[Co(dpgBF_2)_2(OH_2)_2]$,[14] $[CoH(dmgH)_2PBu_3]$,[15] *p*-cyanoanilinium tetrafluoroborate,[6] and triethylammonium tetrafluoroborate[16] were prepared as previously described. Trifluoroacetic acid (Janssen Chimica), tetrafluoroboric acid diethyl ether complex (Fluka), and Et_3NHCl (Acros) were used as received.

Methods and Instrumentation. Electrochemical measurements were carried out under nitrogen. A standard three-electrode configuration was used consisting of a glassy carbon (3 mm in diameter) or platinum (2 mm in diameter) disk as the working electrode, an auxiliary platinum wire, and an Ag/AgCl/aqueous $AgCl_{sat}$ + KCl (3 mol·L^{-1}; hereafter named Ag/AgCl) reference electrode closed by a Vicor frit and directly dipped into the solution. In order to take the liquid junction potential between the aqueous and nonaqueous solution into account, this electrode was calibrated with the internal reference system Fc^+/Fc, which was found at 0.46 V vs Ag/AgCl in CH_3CN (0.53 V vs in DMF). The Fc^+/Fc couple (E^0 = 0.400 V vs SHE)[17] can be used to quote potentials to SHE, when needed.

Cyclic voltammograms were recorded on a EG&G PAR 273A instrument. Solution concentrations were ca. 1 mM for the cobaloxime and 0.1 M for the supporting electrolyte $(n\text{-}Bu_4N)BF_4$. Electrodes were polished on a MD-Nap polishing pad with a 1 μm monocrystalline diamond DP suspension.

Et_3NHBF_4 and *p*-cyanoanilinium tetrafluoroborate were added as solids, trifluoroacetic acid, HBF_4·Et_2O (0.2 mol·L^{-1} solution in the given solvent), and Et_3NHCl (0.05 mol·L^{-1} solution in the given solvent) by syringe. Voltammograms of the supporting electrolyte in CH_3CN and of CH_3CN solutions of Et_3NHCl, CF_3COOH, and *p*-cyanoanilinium tetrafluoroborate in the presence of the supporting electrolyte are given as Supporting Information. Bulk electrolysis and coulometry were carried out on a EG&G PAR 273A instrument in acetonitrile, using a mercury pool cathode. The platinum grid + carbon foam counter electrode was placed in a separated compartment connected with a glass frit and filled with a 0.1 mol·L^{-1} solution of $(n\text{-}Bu_4N)BF_4$ in degassed acetonitrile. A degassed acetonitrile solution (10 mL) containing 0.1 mol·L^{-1} $(n\text{-}Bu_4N)BF_4$ and 0.1 mol·L^{-1} of the acid studied was first electrolyzed at the given potential for 1 h. The catalyst was added as a solid to reach a final concentration of 1 mmol·L^{-1}, and electrolysis was then performed. Hydrogen was tested for purity using a Delsi Nermag DN200 gas chromatograph equipped with a thermal conductivity detector.

Cyclic voltammograms were simulated using DigiElch software.[18] A first simulation and best fitting was performed for $[Co(dmgBF_2)_2(CH_3CN)_2]$ in CH_3CN in the absence of added acid.

(5) (a) Gloaguen, F.; Lawrence, J. D.; Rauchfuss, T. B. *J. Am. Chem. Soc.* **2001**, *123*, 9476. (b) Gloaguen, F.; Lawrence, J. D.; Rauchfuss, T. B.; Bénard, M.; Rohmer, M.-M. *Inorg. Chem.* **2002**, *41*, 6573. (c) Zhao, X.; Georgakaki, I. P.; Miller, M. L.; Yarbrough, J. C.; Darensbourg, M. Y. *J. Am. Chem. Soc.* **2001**, *123*, 9710. (d) Zhao, X.; Georgakaki, I. P.; Miller, M. L.; Mejia-Rodriguez, R.; Chiang, C.-Y.; Darensbourg, M. Y. *Inorg. Chem.* **2002**, *41*, 3917. (e) Georgakaki, I. P.; Miller, M. L.; Darensbourg, M. Y. *Inorg. Chem.* **2003**, *42*, 2489. (f) Chong, D.; Georgakaki, I. P.; Mejia-Rodriguez, R.; Sanabria-Chinchilla, J.; Soriaga, M. P.; Darensbourg, M. Y. *Dalton Trans.* **2003**, 4158. (g) Meija-Rodriguez, R.; Chong, D.; Reibenspies, J. H.; Soriaga, M. P.; Darensbourg, M. Y. *J. Am. Chem. Soc.* **2004**, *126*, 12004. (h) Borg, S. J.; Behrsing, T.; Best, S. P.; Razavet, M.; Liu, X.; Pickett, C. J. *J. Am. Chem. Soc.* **2004**, *126*, 16988. (i) Tard, C.; Liu, X.; Ibrahim, S. K.; Bruschi, M.; De Gioia, L.; Davies, S. C.; Yang, X.; Wang, L.-S.; Sawers, G.; Pickett, C. J. *Nature* **2005**, *433*, 610. (j) Ott, S.; Kritikos, M.; Ackermark, B.; Sun, L.; Lomoth, R. *Angew. Chem., Int. Ed.* **2004**, *43*, 1006. (k) Perra, A.; Davies, E. S.; Hyde, J. R.; Wang, Q.; McMaster, J.; Schröder, M. *Chem. Commun.* **2006**, 1103. (l) Oudart, Y.; Artero, V.; Pécaut, J.; Fontecave, M. *Inorg. Chem.* **2006**, *45*, 4334.

(6) Appel, A.; DuBois, D. L.; Rakowski DuBois, M. *J. Am. Chem. Soc.* **2005**, *127*, 12717.

(7) Wilson, A. D.; Newell, R. H.; McNevin, M. J.; Muckerman, J. T.; Rakowski DuBois, M.; DuBois, D. L. *J. Am. Chem. Soc.* **2006**, *128*, 358.

(8) (a) Kölle, U.; Grützel, M. *Angew. Chem., Int. Ed. Engl.* **1987**, *26*, 567. (b) Kölle, U.; Kang, B.-S.; Infelta, P.; Comte, P.; Grätzel, M. *Chem. Ber.* **1989**, *122*, 1869. (c) Cosnier, S.; Deronzier, A.; Vlachopoulos, N. *J. Chem. Soc., Chem. Commun.* **1989**, 1259.

(9) Connolly, P.; Espenson, J. H. *Inorg. Chem.* **1986**, *25*, 2684.

(10) Hawecker, J.; Lehn, J.-M.; Ziessel, R. *Nouv. J. Chim.* **1983**, *7*, 271.

(11) Part 1 of the series: Razavet, M.; Artero, V.; Fontecave, M. *Inorg. Chem.* **2005**, *44*, 4786.

(12) Hu, X.; Cossairt, B. M.; Brunschwig, B. S.; Lewis, N. S.; Peters, J. C. *Chem. Commun.* **2005**, 4723.

(13) Bakac, A.; Espenson, J. H. *J. Am. Chem. Soc.* **1984**, *106*, 5197.

(14) Tovrog, B. S.; Kitko, D. J.; Drago, R. S. *J. Am. Chem. Soc.* **1976**, *98*, 5144.

(15) Schrauzer, G. N.; Holland, R. J. *J. Am. Chem. Soc.* **1971**, *93*, 1505.

(16) Mohamed, K. S.; Padma, D. K. *Indian J. Chem.* **1988**, *27A*, 759.

(17) Koepp, H. M.; Wedt, H.; Strehlow, H. *Z. Elektrochem.* **1960**, *64*, 483.

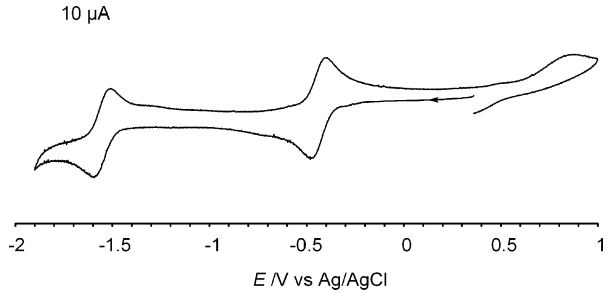

Figure 1. Cyclic voltammogram of $[Co(dmgBF_2)_2(CH_3CN)_2]$ (1×10^{-3} mol·L^{-1}) recorded in a CH_3CN solution of *n*-Bu_4NBF_4 (0.1 mol·L^{-1}) on a glassy carbon electrode at 100 mV·s^{-1} (potentials vs Ag/AgCl).

Parameters were refined until voltammograms recorded at 50, 100, and 500 mV·s^{-1} could be simulated using the same set of values. The resulting parameters were kept unchanged for simulation of voltammograms recorded in the presence of acid. The model was then modified to include the catalytic steps and the new parameters refined until one set of values could provide correct simulation of the voltammograms recorded in the presence of various amounts of added acid (1.5, 3, and 10 equiv) at different scan rates (50, 100, and 500 mV·s^{-1}).

Results

Stability of $[Co(dmgBF_2)_2L]$ (L = CH_3CN, DMF, H_2O) in the Presence of Acids. The spectrum of $[Co(dmgBF_2)_2(OH_2)_2]$ in CH_3CN (DMF) displays an absorption maximum at 420 (460) nm. In the noncoordinating solvent $CHCl_3$, the maximum absorbance is at $\lambda_{max} = 440$ nm. The addition of a few microliters of CH_3CN (DMF) to this solution leads to a shift of this maximum absorbance to 420 (460) nm, indicating displacement of the coordinated water molecules by CH_3CN (DMF). In the following, the complexes will then be written as $[Co(dmgBF_2)_2L]$ (L = CH_3CN or DMF), even if it is not precisely known whether the complex in the solution is penta- or hexacoordinated with one very labile axial ligand.[13]

The stability of millimolar solutions of $[Co(dmgBF_2)_2L]$ in the presence of acids (30 equiv) was monitored spectrophotometrically by following the decay of the maximum absorbance. $[Co(dmgBF_2)_2L]$ proved stable over days in the presence of Et_3NHBF_4 or Et_3NHCl. In the presence of CF_3COOH, however, the complex decomposes with half-lives of 2 days in CH_3CN and 3 days in DMF approximately. Degradation is even faster with *p*-cyanoanilinium tetrafluoroborate ($t_{1/2}$ = 15 h and 1 day, respectively). As reported by Peters et al.,[12] stronger acids such as HCl·Et_2O and HBF_4·Et_2O hydrolyze $[Co(dmgBF_2)_2L]$ within a few minutes in acetonitrile. After the reaction, the solution does not display any absorption in the visible spectrum. The same behavior is observed in DMF for HCl·Et_2O, but the hydrolysis is slower in the case of HBF_4·Et_2O ($t_{1/2}$ = 15 h). Further studies are needed to characterize the degradation product.

Cyclic Voltammogram of $[Co(dmgBF_2)_2L]$. The cyclic voltammogram (Figure 1 and the Supporting Information) and rotating disk electrode (RDE) steady-state voltammogram (see the Supporting Information) of $[Co(dmgBF_2)_2L]$ recorded on a glassy carbon electrode exhibit two well-defined one-electron waves with chemically reversible characteristics. The first process at −0.44 V vs Ag/AgCl or −0.50 V vs SHE in acetonitrile (−0.51 V vs Ag/AgCl or −0.64 V vs SHE in DMF) is generally assigned to the Co^{II}/Co^{I} couple in the literature.[9,12,19] This potential value is in good agreement with that of −0.43V vs SHE previously reported by Connolly and Espenson.[9] The second process at −1.55 V vs Ag/AgCl in acetonitrile (−1.44 V vs Ag/AgCl in DMF) could correspond to either a metal or a ligand-centered reduction. Spectroscopic characterization of the one-electron- and two-electron-reduced species using UV−visible spectroscopy and electron paramagnetic resonance proved impossible because both compounds are unstable at room temperature in CH_3CN or DMF solution at the time scale of electrolysis.

A one-electron oxidative process is furthermore observed with $E_{pa} = 0.95$ V and $E_{pc} = 0.26$ V vs Ag/AgCl in CH_3CN ($E_{pa} = 0.74$ and $E_{pc} = 0.30$ V vs Ag/AgCl in DMF). These waves are not clearly defined but reveal some chemical reversibility. This process could be tentatively assigned to the Co^{III} oxidation state by comparison with the electrochemical behavior of the parent cobaloxime $[Co(dmgH)_2pyCl]$.[11]

Cyclic Voltammograms of $[Co(dmgBF_2)_2L]$ in the Presence of Acids. Cyclic voltammograms of $[Co(dmgBF_2)_2L]$ were recorded over the potential range from +1.0 to −1.9 V vs Ag/AgCl in CH_3CN and DMF in the presence of 1.5, 3, and 10 equiv of different acids:[20] tetrafluoroboric acid diethyl ether complex (pK_a = 0.1 in CH_3CN),[12] *p*-cyanoanilinium tetrafluoroborate (pK_a = 7.6 in CH_3CN),[20b] trifluoroacetic acid (pK_a = 12.7 in CH_3CN), and triethylammonium tetrafluoroborate (pK_a = 18.7 in CH_3CN and 10.7 in DMF). The values of the calculated standard potentials[21] and experimental electrocatalytic reduction potentials of these acids on a glassy carbon electrode in the presence of a cobaloxime as a catalyst or on a platinum electrode are given in Table 1. These values will be commented upon in the Discussion section. In the following, only the electrocatalytic waves of the cyclic voltammograms will be considered even though less intense signals following these waves are also observed. These signals are also found in cyclic voltammograms recorded on platinum or glassy carbon electrodes in the absence of a cobalt catalyst. They may correspond to the reduction of minor protonated solvent species, the exact nature of which is not definitively known, and are not directly related with the electrocatalyzed process under study.

(a) Strong-Acid Behavior. As reported by Peters et al.,[12] the addition of a relatively strong acid such as *p*-cyano-

(18) (a) Rudolph, M. *J. Electroanal. Chem.* **2003**, *543*, 23. (b) Rudolph, M. *J. Electroanal. Chem.* **2003**, *558*, 171. (c) Rudolph, M. *J. Electroanal. Chem.* **2004**, *571*, 289. (d) Rudolph, M. *J. Comput. Chem.* **2005**, *26*, 619. (e) Rudolph, M. *J. Comput. Chem.* **2005**, *26*, 633. (f) Rudolph, M. *J. Comput. Chem.* **2005**, *26*, 1193.

(19) Campbell, C. J.; Haddleton, D. M.; Rusling, J. F. *Electrochem. Commun.* **1999**, *1*, 618.

(20) (a) Izutsu, K. *Acid−Base Dissociation Constants in Dipolar Aprotic Solvents*; Blackwell Scientific Publications: Oxford, U.K., 1990. (b) Edidin, R. T.; Sullivan, J. M.; Norton, J. R. *J. Am. Chem. Soc.* **1987**, *109*, 3945.

(21) Felton, G. A. N.; Glass, R. S.; Lichtenberger, D. L.; Evans, D. H. *Inorg. Chem.* **2006**, *45*, 9181.

Table 1. Hydrogen Evolution Potentials vs Ag/AgCl/KCl_{aq} 3 mol·L^{-1} on Glassy Carbon in the Presence of Various Cobaloximes and Platinum for Different Acids

acid	solvent	standard potential[21]/V	E_{her} on platinum/V	cobaloxime-catalyzed E_{her} on glassy carbon/V	catalyst	$E°(Co^{II}/Co^{I})$/V	ref
Et_3NH^+	DMF	−0.78	−0.95	−0.98	$[Co(dmgH)_2pyCl]$	−0.98	11
CF_3COOH	CH_3CN	−0.43	−0.43	−0.43	$[Co(dmgBF_2)_2L]$	−0.44	12 and this work
p-cyanoanilinium	CH_3CN	−0.13	−0.15	−0.34	$[Co(dmgBF_2)_2L]$	−0.44	this work
p-cyanoanilinium	DMF		−0.35	−0.52	$[Co(dmgBF_2)_2L]$	−0.51	this work
$HCl·Et_2O$	CH_3CN	−0.21	−0.26	−0.28	$[Co(dpgBF_2)_2L]$ [a]	−0.29	12
$HBF_4·Et_2O$	DMF		−0.34	−0.52	$[Co(dmgBF_2)_2L]$	−0.51	this work

[a] $dpgBF_2^-$ = (difluoroboryl)diphenylglyoximato anion.

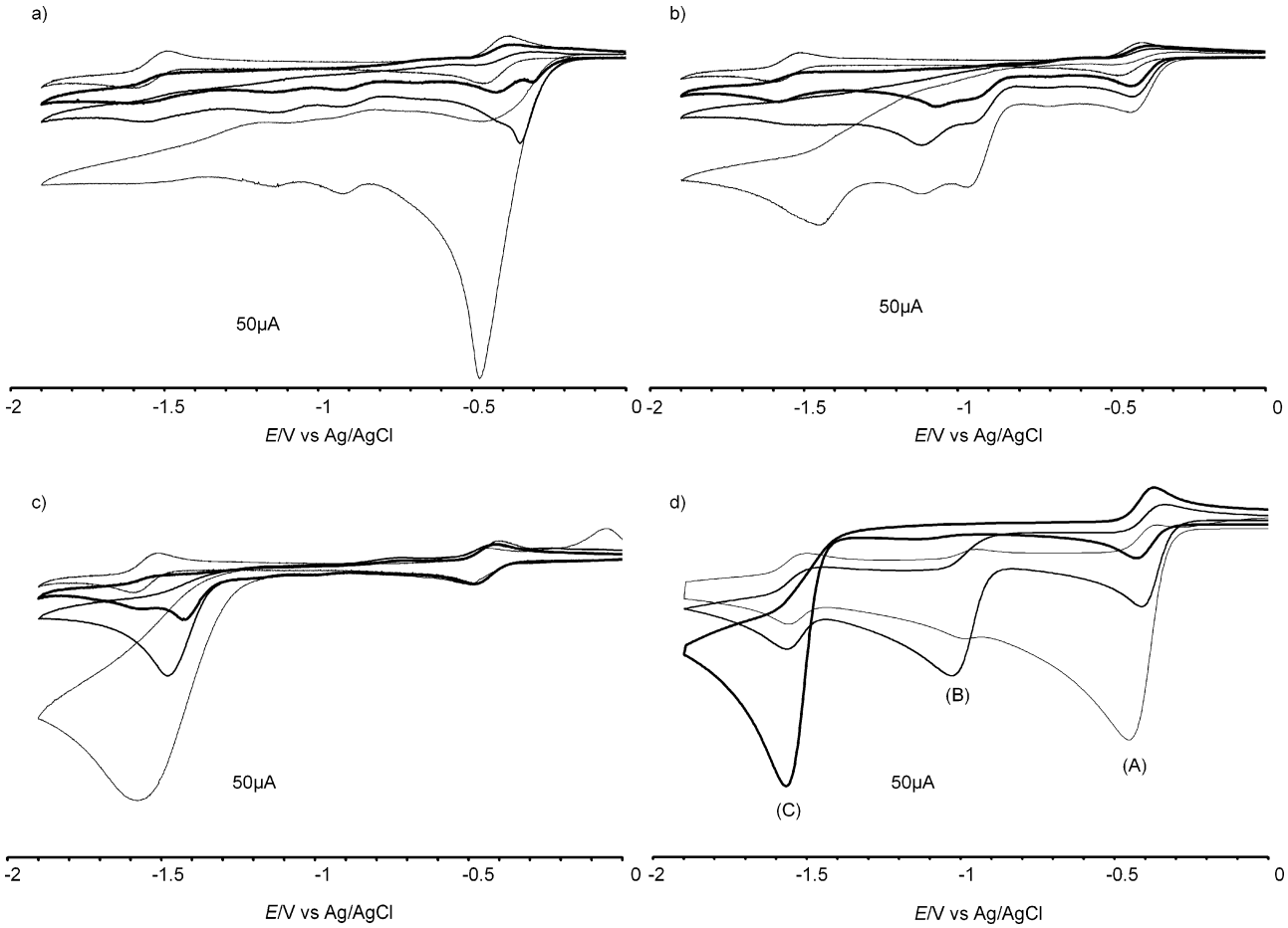

Figure 2. Cyclic voltammograms of $[Co(dmgBF_2)_2(CH_3CN)_2]$ (1.10^{-3} mol·L^{-1}) recorded in a CH_3CN solution of *n*-Bu_4NBF_4 (0.1 mol·L^{-1}) on a glassy carbon electrode at 100 mV·s^{-1} in the presence of (top to bottom) 0, 1.5, 3.0, and 10 equiv of (a) *p*-cyanoanilinium tetrafluoroborate, (b) CF_3COOH, (c) and Et_3NHCl. (d) Simulated cyclic voltammograms of $[Co(dmgBF_2)_2(CH_3CN)_2]$ (1×10^{-3} mol·L^{-1}) at 100 mV·s^{-1} in the presence of 10 equiv of (A) *p*-cyanoanilinium tetrafluoroborate, (B) CF_3COOH, and (C) Et_3NHCl (potentials vs Ag/AgCl).

anilinium tetrafluoroborate to a solution of $[Co(dmgBF_2)_2L]$ in CH_3CN (or $HBF_4·Et_2O$ to a solution of $[Co(dmgBF_2)_2L]$ in DMF) triggers the appearance of a new irreversible cathodic wave near the Co^{II}/Co^{I} response (Figure 2a). This behavior is typical for a "total" catalysis for hydrogen evolution:[22] At low acid/catalyst concentration ratios, the catalytic wave lies at more positive potentials (−0.344 V vs Ag/AgCl) than that of the Co^{II}/Co^{I} couple. Increasing the acid/catalyst concentration ratio raises the height of the new wave and shifts it to more negative potentials while the Co^{II}/Co^{I} reversible wave disappears. This behavior is similar to that previously observed for proton reduction catalyzed by $[Co(dmgH)_2(py)Cl]$ in DMF,[11] which suggests that the mechanism (Scheme 1, pathway i) involves a first reduction step. The protonation of $[Co^{I}(dmgBF_2)_2L]^-$ then produces a cobalt(III) hydride species as an intermediate, which is proposed in Scheme 1 to evolve hydrogen heterolytically (see the Discussion section). The initial species is regenerated by a last electron-transfer step.

(b) Weak-Acid Behavior. By contrast, the addition of a weak acid such as Et_3NHCl to a solution of $[Co(dmgBF_2)_2L]$ in CH_3CN (Figure 2c) or DMF leads to the appearance of a similar catalytic wave but located near the $[Co(dmgBF_2)_2L]^-/[Co(dmgBF_2)_2L]^{2-}$ process at −1.43 V vs Ag/AgCl. It should be noted that around 20% of the current measured at the

(22) (a) Andrieux, C. P.; Blocman, C.; Dumas-Bouchiat, J.-M.; M'Halla, F.; Savéant, J.-M. *J. Electroanal. Chem.* **1980**, *113*, 19. (b) Savéant, J.-M.; Su, K. B. *J. Electroanal. Chem.* **1984**, *171*, 341.

Scheme 1. Catalytic Mechanisms for Electrocatalyzed Hydrogen Evolution

Mechanism (i)

$[Co^{II}(dmgBF_2)_2L] + e^- \rightleftharpoons [Co^{I}(dmgBF_2)_2L]^-$

$[Co^{I}(dmgBF_2)_2L]^- + H^+ \rightleftharpoons [Co^{III}H(dmgBF_2)_2L]$

$[Co^{III}H(dmgBF_2)_2L] + H^+ \rightleftharpoons [Co^{III}(dmgBF_2)_2L]^+ + H_2$

$[Co^{III}(dmgBF_2)_2L]^+ + e^- \rightleftharpoons [Co^{II}(dmgBF_2)_2L]$

Mechanism (ii)

$[Co^{II}(dmgBF_2)_2L] + e^- \rightleftharpoons [Co^{I}(dmgBF_2)_2L]^-$

$[Co^{I}(dmgBF_2)_2L]^- + H^+ \rightleftharpoons [Co^{III}H(dmgBF_2)_2L]$

$[Co^{III}H(dmgBF_2)_2L] + e^- \rightleftharpoons [Co^{II}H(dmgBF_2)_2L]^-$

$[Co^{II}H(dmgBF_2)_2L]^- + H^+ \rightleftharpoons [Co^{II}(dmgBF_2)_2L] + H_2$

$2\,[Co^{II}H(dmgBF_2)_2L]^- \rightleftharpoons 2\,[Co^{I}(dmgBF_2)_2L]^- + H_2$

Mechanism (iii)

$[Co^{II}(dmgBF_2)_2L] + e^- \rightleftharpoons [Co^{I}(dmgBF_2)_2L]^-$

$[Co^{I}(dmgBF_2)_2L]^- + e^- \rightleftharpoons [Co(dmgBF_2)_2L]^{2-}$

$[Co(dmgBF_2)_2L]^{2-} + H^+ \rightleftharpoons [Co^{II}H(dmgBF_2)_2L]^-$

$[Co^{II}H(dmgBF_2)_2L]^- + H^+ \rightleftharpoons [Co^{II}(dmgBF_2)_2L] + H_2$

$2\,[Co^{II}H(dmgBF_2)_2L]^- \rightleftharpoons 2\,[Co^{I}(dmgBF_2)_2L]^- + H_2$

peak potential for 10 equiv of Et_3NHCl in Figure 2c is due to the direct reduction of Et_3NH^+ at the glassy carbon electrode. This catalytic process may involve a heterolytic mechanism (Scheme 1, pathway iii) as in the case of pathway i but involving a cobalt(II) hydride intermediate instead of the cobalt(III) hydride species. However, a homolytical reaction of the cobalt(II) hydride intermediate cannot be excluded.

(c) Intermediate-Acid Behavior. The addition of acids with intermediate strength, such as CF_3COOH in CH_3CN (Figure 2b) or $HBF_4{\cdot}Et_2O$ and *p*-cyanoanilinium tetrafluoroborate in DMF (see the Supporting Information),[23] results in another modification of the cyclic voltammograms of $[Co(dmgBF_2)_2L]$ (Figure 2b): A catalytic behavior is still observed near the Co^{II}/Co^{I} response but with lower current intensity and thus a slower overall reaction rate. In addition, a new irreversible cathodic wave appears near −1.0 V vs Ag/AgCl, the height of which rises upon increasing acid concentration. As far as the mechanism is concerned (Scheme 1, pathway ii), the presence of this new catalytic wave may indicate that the cobalt(III) hydride involved as a catalytic intermediate in pathway i had not totally reacted and could be electrochemically reduced at this potential value (−1.0 V vs Ag/AgCl), producing the active species for the second catalytic wave. This new intermediate was formally written as cobalt(II) hydride, which can evolve hydrogen by parallel heterolytic and hemolytic pathways. This mechanism parallels that established by Savéant et al. for the reduction of $CNCH_2COOH$ catalyzed by the rhodium porphyrin complex $[Rh(TPP)I(PPh_3)]$.[24]

Scheme 2. Mechanistic Scheme Used for Modeling of Cyclic Voltammograms

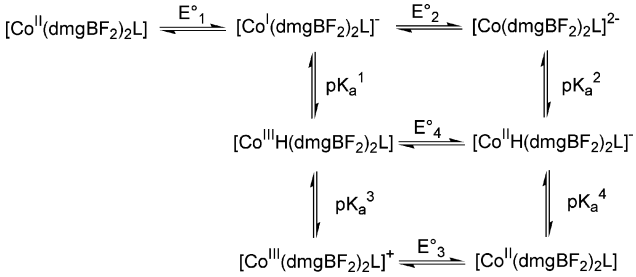

Scheme 3. Definition of Acid Dissociation Constants pK_a^{1-4}

$[Co^{III}H(dmgBF_2)_2L] \rightleftharpoons [Co^{I}(dmgBF_2)_2L]^- + H^+ \quad pK_a^1$

$[Co^{II}H(dmgBF_2)_2L]^- \rightleftharpoons [Co(dmgBF_2)_2L]^{2-} + H^+ \quad pK_a^2$

$[Co^{III}(dmgBF_2)_2L]^+ + H_2 \rightleftharpoons [Co^{III}H(dmgBF_2)_2L] + H^+ \quad pK_a^3$

$[Co^{II}(dmgBF_2)_2L] + H_2 \rightleftharpoons [Co^{II}(dmgBF_2)_2L]^- + H^+ \quad pK_a^4$

Table 2. Thermodynamic Parameters Extracted from Simulation of the Voltammograms (*E*/V vs Ag/AgCl)

$[CoH(dmgBF_2)_2L]/[Co(dmgBF_2)_2L]^-$	$pK_a^1 = 13.3$
$[CoH(dmgBF_2)_2L]^-/[Co(dmgBF_2)_2L]^{2-}$	$pK_a^2 = 23.0$
$[Co(dmgBF_2)_2L]^+ + H_2/[CoH(dmgBF_2)_2L]$	$pK_a^3 = 10.5$
$[Co(dmgBF_2)_2L] + H_2/[CoH(dmgBF_2)_2L]^-$	$pK_a^4 = 36.3$
$[CoH(dmgBF_2)_2L]/[CoH(dmgBF_2)_2L]^-$	$E° = -0.98$ V

Cyclic Voltammograms Modeling. In order to confirm the proposed pathways for *her*, we have modeled the cyclic voltammograms for the electrocatalyzed reduction of *p*-cyanoanilinium tetrafluoroborate, CF_3COOH, and Et_3NHCl in CH_3CN using the DigiElch software.[18]

In a first approach, only the heterolytic pathways leading to dihydrogen from both $Co^{III}-H$ and $Co^{II}-H$ were input in the modelization. Pathways i−iii used for modeling the different catalytic behaviors form, in fact, two fused square schemes as shown in Scheme 2. Whereas the electrochemical parameters ($E°_1$, $E°_2$, and $E°_3$) for $[Co(dmgBF_2)_2L]$ could be determined from voltammograms recorded in the absence of acid, the four thermodynamic acidity constants (pK_a^{1-4}) and the electrochemical potential $E°_4$ of the $[CoH(dmgBF_2)_2L]/[CoH(dmgBF_2)_2L]^-$ couple (Scheme 1, pathway ii) were unknown. The presence of two square schemes in the mechanism (Scheme 2) finally reduces to three the number of independent constants, and we chose the three acid−base couple pK_a values $[CoH(dmgBF_2)_2L]/[Co(dmgBF_2)_2L]^-$ (pK_a^1), $[CoH(dmgBF_2)_2L]^-/[Co(dmgBF_2)_2L]^{2-}$ (pK_a^2), and $[Co(dmgBF_2)_2L]^+ + H_2/[CoH(dmgBF_2)_2L]$ (pK_a^3) defined in Scheme 3 using the classical formalism for acid dissociation reactions. We succeeded in modeling all of the cyclic voltammograms recorded at 50, 100, and 500 $mV{\cdot}s^{-1}$ in the presence of 1.5, 3, and 10 equiv of the three acids with one set of thermodynamic constants (Table 2) and thus were able to reproduce the three different electrocatalytic behaviors (Figure 2d and the Supporting Information).[25] The derived potential for $[CoH(dmgBF_2)_2L]/[CoH(dmgBF_2)_2L]^-$ (−0.98

(23) DMF is indeed known to strongly solvate protons and thus to level down the strength of the acids. Tremillon, B. *Chemistry in non-aqueous solvents*; D. Reidel Publishing Co.: Dordrecht, The Netherlands, 1971.

(24) Grass, V.; Lexa, D.; Savéant, J.-M. *J. Am. Chem. Soc.* **1997**, *119*, 7526.

V vs Ag/AgCl in CH_3CN) is in the same range as that measured in DMF (−0.78 V vs Ag/AgCl) on an authentic sample of $[CoH(dmgH)_2PBu_3]/[CoH(dmgH)_2PBu_3]^-$.[15] The pK_a values determined in CH_3CN for $[CoH(dmgBF_2)_2L]/[Co(dmgBF_2)_2L]^-$ and $[Co(dmgBF_2)_2L]^+ + H_2/[CoH(dmgBF_2)_2L]$ are very similar to those calculated from our previously published data:[11] 15.4 for $[CoH(dmgH)_2py]/[Co(dmgH)_2py]^-$ and 16.3 for $[Co(dmgH)_2py]^+ + H_2/[CoH(dmgH)_2py]$ in DMF.

Further simulations of cyclic voltammograms were carried out using a hemolytic model consisting of a bimolecular reductive elimination generating dihydrogen from either two $Co^{III}-H$ or two $Co^{II}-H$ species.

In the first case, we found it impossible to simulate the differences observed between strong and intermediate acid conditions. In both cases, the sole catalytic wave observed was the one at −0.35 V vs Ag/AgCl.

In the second case, simulated voltammograms were found unchanged for values of the bimolecular rate constant k_{homo} larger than 10^5 $mol^{-1}\cdot L\cdot s^{-1}$. For comparison, a value of 1.7×10^4 $mol^{-1}\cdot L\cdot s^{-1}$ was determined for the rate constant of homolytic hydrogen evolution from $[HCo(dmgH)_2PBu_3]$.[26] The introduction of both heterolytical and homolytical pathways in the model resulted in similar cyclic voltammograms.

Bulk Electrolysis Experiments for Hydrogen Evolution. Bulk electrolysis for hydrogen evolution, coupled to hydrogen titration, using $[Co(dmgBF_2)_2L]$ as the catalyst was already reported in the presence of Et_3NHBF_4 (−0.9 V vs Ag/AgCl in DMF, 4.7 TON·h^{-1}, 80 TON)[11] and CF_3COOH (−0.72 V vs SCE, 20 TON·h^{-1}, 20 TON).[12] In both cases, the faradaic yield was almost quantitative. In order to sort the various conditions (nature of the acid and applied potential) regarding turnover frequencies, bulk electrolysis experiments were undertaken using the same experimental procedure. A mercury pool cathode was chosen in order to minimize the reduction current for the uncatalyzed reduction of Et_3NH^+ at −1.6 V vs Ag/AgCl.[21] The evolved hydrogen was characterized by GC analysis. Three values of applied potentials (−0.5, −1.0, and −1.6 V vs Ag/AgCl) were chosen, corresponding to the electrocatalytic potentials observed in cyclic voltammograms. Figure 3 shows the evolution of the total charge passed as a function of time during 1 h of bulk electrolysis of solutions containing $[Co(dmgBF_2)_2L]$ in the presence of 100 equiv of acid. Catalytic reduction of Et_3NHCl (Figure 3, traces c and e) was significantly faster when the applied potential was set to −1.6 V vs Ag/AgCl, a value corresponding to that of the sole catalytic wave observed by cyclic voltammetry. CF_3COOH was reduced with a higher current at −1.0 V as compared to −0.5 V vs Ag/AgCl (compare Figure 3, traces b and d). $[Co(dmgBF_2)_2L]$ was much more active at −0.5 V vs Ag/AgCl toward *p*-cyanoanilinium tetrafluoroborate compared to CF_3COOH. The reduction of *p*-cyanoanilinium tetrafluoroborate was almost finished (46 TON, 92% conversion based on coulometry) after 30 min at −0.5 V vs Ag/AgCl corresponding to a turnover frequency of 92 TON·h^{-1}.

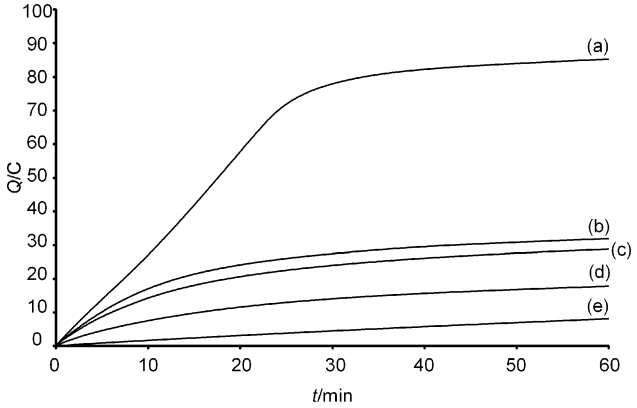

Figure 3. Coulometry for bulk electrolysis of a CH_3CN solution (10 mL) of various acids (0.1 mol·L^{-1}) and n-Bu_4NBF_4 (0.1 mol·L^{-1}) at a mercury pool electrode in the presence of 1×10^{-3} mol·L^{-1} $[Co(dmgBF_2)_2(CH_3CN)_2]$ at different potentials: (a) *p*-cyanoanilinium tetrafluoroborate/−0.5 V, (b) CF_3COOH/−1.0 V, (c) Et_3NHCl/−1.6 V, (d) CF_3COOH/−0.5 V, and (e) Et_3NHCl/−1.0 V vs Ag/AgCl [1 turnover ($2e^-$/catalyst) corresponds to 1.93 C].

We have, furthermore, observed that an exhaustive electrolysis of CH_3CN solutions of $[Co(dmgBF_2)_2L]$ at either −0.5 or −1.6 V vs Ag/AgCl in the absence of acid results in the loss of catalytic properties of the complex: when, in a second step, acid is added to the solution and a potential (−0.5, −1.0, or −1.6 V vs Ag/AgCl) is applied, no catalytic current could be measured. In the same manner, the species formed by acidic degradation of $[Co(dmgBF_2)_2L]$ was found to be catalytically inactive. This indicates that, because of fast turnover cycling in the presence of acid, the reduced catalyst is protected against decomposition.

Discussion

Hydrogen Evolution Mechanism. Metal−hydride species are classical intermediates of the hydrogen evolution reaction. Their catalytic implication was demonstrated in a great number of catalytic systems such as those based on metal porphyrins (M = Fe,[27] Co,[28] and Rh[24]), cyclopentadienyl complexes of cobalt[29] and rhodium,[8] $[Ni(P^{Ph}_2N^{Ph}_2)_2(CH_3CN)](BF_4)_2$ ($P^{Ph}_2N^{Ph}$ = 1,3,5,7-tetraphenyl-1,5-diaza-3,7-diphosphacyclooctane),[6] or diiron mimicks of iron-only hydrogenases.[5] Co−H species are commonly proposed as intermediates in cobaloxime-catalyzed evolution of molecular hydrogen[9,11,12] on the basis of the known reactivity of isolated hydridocobaloximes.[26]

Most of the molecular complexes reported so far are active for proton electroreduction under only one redox state. A notable exception is given by the rhodium tetraphenylporphyrin system in which all three $[Rh^{II}H(TPP)]$, $[Rh^{III}H(TPP)(PPh_3)]$, and $[Rh^{II}H(TPP)(PPh_3)]$ species catalyze $CNCH_2$-

(25) For these simulations, the new electrochemical kinetic parameters ($Co^{III}-H/Co^{II}-H$ couple) were fixed at standard values and were not best-fitted. In contrast, the chemical kinetic parameters that influence both the potential (EC processes) and the heights of the electrocatalytic waves were adjusted during simulation (see the Supporting Information).

(26) Chao, T.-H.; Espenson, J. H. *J. Am. Chem. Soc.* **1978**, *100*, 129.

(27) Bhugun, I.; Lexa, D.; Savéant, J.-M. *J. Am. Chem. Soc.* **1996**, *118*, 3982.

(28) Kellett, R. M.; Spiro, T. G. *Inorg. Chem.* **1985**, *24*, 2373, 2378.

(29) Koelle, U.; Ohst, S. *Inorg. Chem.* **1986**, *25*, 2689.

CO_2H reduction whereas [$Rh^{III}H$(TPP)] does not.[24] The results described in this paper highlight three different pathways for hydrogen evolution electrocatalyzed by the same complex, [Co(dmgBF_2)$_2$L], in nonaqueous solvents, depending on the strength of the acid used. They can be described starting from the Co^{II} state (Scheme 1) as follows: (i) an ECCE mechanism involving Co^{III}−H as the active species, (ii) an ECEC mechanism involving both Co^{III}−H and Co^{II}−H as intermediates, and (iii) an EECC mechanism involving Co^{II}−H as the active species.

Hydrogen evolution proceeds via pathway i if the acid used is strong enough to protonate both [Co^{I}(dmgBF_2)$_2$L]$^-$ and [Co^{III}H(dmgBF_2)$_2$L]. With acids of lower strength, the Co^{III}−H intermediate cannot be protonated and is thus further reduced to produce the electrocatalytic Co^{II}−H intermediate (pathway ii). Finally, very weak acids such as Et_3NH^+ do not protonate [Co^{I}(dmgBF_2)$_2$L]$^-$ but are able to react with the very nucleophilic [Co(dmgBF_2)$_2$L]$^{2-}$, which mediates hydrogen evolution (pathway iii) below −1.4 V vs Ag/AgCl.

The reactivity reported by Peters et al. using trifluoroacetic acid occurs at the Co^{II}/Co^{I} process and thus proceeds via pathway i.[12] We could show that this acid is also reduced via pathway ii at −0.97 V vs Ag/AgCl. This means that the diffusion layer is not fully depleted in acid at the end of the first catalytic wave and thus that this first process is not that fast. Indeed, *p*-cyanoanilinium is reduced much more efficiently (i.e., with higher currents in similar conditions) via pathway i.

We can, moreover, understand why, as we reported previously, [Co(dmgBF_2)$_2$L] catalyzes Et_3NH^+ reduction slowly in 1,2-dichloroethane at −0.9 V vs Ag/AgCl (and not at higher potentials):[11] A small signal assigned to [CoH(dmgBF_2)$_2$L]/[CoH(dmgBF_2)$_2$L]$^-$ is seen at −0.9 V vs Ag/AgCl in the cyclic voltammogram of [Co(dmgBF_2)$_2$L] in the presence of Et_3NH^+ (Figure 2). Thus, bulk electrolysis produces [Co(dmgBF_2)$_2$L]$^-$, which accumulates in the bulk and is partially protonated to form [CoH(dmgBF_2)$_2$L]. The latter is electrochemically reduced to yield [CoH(dmgBF_2)$_2$L]$^-$. Hydrogen evolution catalysis proceeds via pathway ii. With the first protonation step being thermodynamically strongly unfavored and acting as a bottleneck for the reaction, the turnover frequency was too low compared to the cyclic voltammetry time scale for the electrocatalytic wave to be observed using this technique.

Metal hydride can evolve hydrogen through two main mechanisms: (i) hydride protonation leading to the heterolytic cleavage of the M−H bond and (ii) reductive elimination from two complexes through the homolytic cleavage of the M−H bond. For example, the hydridocobaloxime [Co(dmgH)$_2$(PBu_3)H] evolves dihydrogen by parallel heterolytic and homolytic mechanisms.[26] We could demonstrate that the Co^{III}−H intermediate (pathway i) mediates only heterolytic dihydrogen production in the same manner as [CoH(dmgH)$_2$py].[11] In contrast, whether hydrogen evolution from the Co^{II}−H species (pathways ii and iii) is heterolytic and/or hemolytic could not be experimentally determined. However, the Co^{II}−H bond should be stronger than the Co^{III}−H bond and thus more resistant to reductive elimination. This general trend is illustrated by the fact that ruthenium(III) porphyrin hydrides easily eliminate dihydrogen while the corresponding anionic ruthenium(II) hydrides are resistant to reductive elimination.[30]

Activation Potential. The $H_2/2H^+ + 2e^-$ interconversion is a two-electron process, and related reactions should involve either a hydrogen radical or a hydride ion. On platinum, palladium, and nickel surfaces, the reduction of protons occurs with low overvoltages (also called activation potential) through a "homolytic" mechanism because of stabilization of adsorbed hydrogen and the reversible desorption of dihydrogen.[4b] In contrast, these reactions always proceed in solution via a "heterolytic" pathway involving a hydride ion stabilized through some chemical interaction with the catalysts.[4] Coordination complexes are thus naturally suited for such a catalysis because they combine both redox and acid−base reactivities. However, by contrast with a metallic material displaying a conduction band with an energy continuum, these complexes can only provide electrons at their redox potentials. Thus, it is not conceivable that a given molecular compound could catalyze electroreduction of protons near equilibrium over the entire pK_a range.

The reactivity of cobaloximes with regard to acid reduction can be tuned by synthetic modifications of the cobalt coordination sphere. Thus, given an acid and knowing its standard potential in the solvent under study,[21] it is possible to find a cobaloxime with comparable Co^{II}/Co^{I} redox potential that catalyzes hydrogen evolution on a carbon electrode in organic solvents with a small activation potential, very close to that observed on platinum (Table 1, lines 1, 2, and 5).

Even if cobaloximes combined with glassy carbon electrodes have small overvoltages for the hydrogen evolution reaction, it is desirable for technological applications to design catalysts with higher Co^{II}/Co^{I} potentials.[4a] However, this will result in a less nucleophilic metal center and, as a consequence, stronger acid will be required for electrocatalytic activity.[4,11] Unfortunately, under these conditions, cobaloximes are significantly hydrolyzed and lose activity. The {BF_2}-bridged cobaloximes are known as the more stable cobaloximes in acidic conditions,[4b,9,13] but, nevertheless, [Co(dmgBF_2)$_2$L] is readily, albeit slowly, hydrolyzed by acids such as *p*-cyanoanilinium (pK_a = 7.6 in CH_3CN) or H_2SO_4 (pK_a = 7.2 in CH_3CN). The same is true for [Co(dpgBF_2)$_2$L] [dpgBF_2^- = (difluoroboryl)diphenylglyoximato anion], which decomposes in the presence of HBF_4·Et_2O.[12] The balance should thus be found between thermodynamics and stability: for example, [Co(dmgBF_2)$_2$L] catalyzes hydrogen evolution more slowly but, because the catalyst is not hydrolyzed, for a longer time in the presence of CF_3COOH as compared to *p*-cyanoanilinium.

Up to last year and with the exception of a rhodium-based electrocatalyst active at −0.55 V vs SCE,[31] all of the first-

(30) Collman, J. P.; Hutchison, J. E.; Wagenknecht, P. S.; Lewis, N. S.; Lopez, M. A.; Guilard, R. *J. Am. Chem. Soc.* **1990**, *112*, 8206. Collman, J. P.; Wagenknecht, P. S.; Hutchison, J. E.; Lewis, N. S.; Lopez, M. A.; Guilard, R.; L'Her, M.; Bothner-By, A. A.; Mishra, P. K. *J. Am. Chem. Soc.* **1992**, *114*, 5654.

row transition-metal series electrocatalysts were active at potentials below −0.90 V vs Ag/AgCl.[11] Two other catalysts active at quite positive potentials were recently described in the litterature, both of them in the presence of strong acids: $[Ni(P^{Ph}_2N^{Ph}_2)_2(CH_3CN)](BF_4)_2$ ($P^{Ph}_2N^{Ph}_2$ = 1,3,5,7-tetraphenyl-1,5-diaza-3,7-diphosphacyclooctane) catalyzes the reduction of triflic acid (pK_a = 2.6 in CH_3CN) at −0.40 vs Ag/AgCl,[7] and $[Cp_2Mo_2(\mu\text{-}S)_2(\eta^2\text{-}\mu_2\text{-}CH_2S_2)]$ mediates hydrogen evolution from *p*-cyanoanilinium (pK_a = 7.6 in CH_3CN) at −0.24 vs Ag/AgCl.[6] Bulk electrolysis experiments for proton electroreduction by $[Ni(P^{Ph}_2N^{Ph}_2)_2(CH_3CN)](BF_4)_2$ and $[Cp_2Mo_2(\mu\text{-}S)_2(\eta^2\text{-}\mu_2\text{-}CH_2S_2)]$ were only carried out up to 6.5 and 10 turnovers, respectively. Despite the fact that the electrocatalytic wave in cyclic voltammograms is observed to be 100 mV more negative than that of $[Cp_2Mo_2(\mu\text{-}S)_2(\eta^2\text{-}\mu_2\text{-}CH_2S_2)]$ under the same conditions, $[Co(dmgBF_2)_2(CH_3CN)_2]$ proved to be much more active as a catalyst during bulk electrolysis experiments at −0.5 V vs Ag/AgCl in CH_3CN because 46 turnovers were achieved within 30 min to be compared to the 10 equiv of hydrogen produced by $[Cp_2Mo_2(\mu\text{-}S)_2(\eta^2\text{-}\mu_2\text{-}CH_2S_2)]$ within 3 h.

(31) (a) Kölle, U.; Grützel, M. *Angew. Chem., Int. Ed. Engl.* **1987**, *26*, 567. (b) Kölle, U.; Kang, B.-S.; Infelta, P.; Comte, P.; Grätzel, M. *Chem. Ber.* **1989**, *122*, 1869. (c) Cosnier, S.; Deronzier, A.; Vlachopoulos, N. *J. Chem. Soc., Chem. Commun.* **1989**, 1259.

Conclusions

$[Co(dmgBF_2)_2L]$ (L = CH_3CN or DMF) is currently one of the most efficient catalysts for hydrogen evolution in a nonaqueous solvent in terms of potential, turnover frequency, and stability. Increasing the electrochemical potential is essential in two perspectives: (i) aqueous application where the −0.413 V vs SHE value for the apparent potential of the H^+/H_2 couple at pH 7 would apply and (ii) interaction with semiconductor photosensitive materials such as TiO_2, which cannot transfer electrons to the catalyst at potentials below that of its conduction band ($E_{1/2}(CB) = -0.11 + 0.059 \times$ pH V vs SHE).[4b] We are currently investigating the properties of $[Co(dmgBF_2)_2(H_2O)_2]$ for proton electroreduction in aqueous conditions.

Acknowledgment. The authors acknowledge the Life Science Division of the Commissariat à l'Energie Atomique for financial support within the Biohydrogen program.

Supporting Information Available: Experimental data and simulations, including parameters, using DigiElch and cyclic voltammograms of supporting electrolyte (blank experiment), *p*-cyanoanilinium tetrafluoroborate, CF_3COOH, and Et_3NHCl. This material is available free of charge via the Internet at http://pubs.acs.org.

IC061625M